Modeling and Simulation of a Large Chipper Drive

Hansjörg Kapeller Anton Haumer Christian Kral Gert Pascoli Franz Pirker
arsenal research
Giefinggasse 2, 1210 Vienna, Austria
hansjoerg.kapeller@arsenal.ac.at

Abstract

This paper presents a simulation model for a large chipper drive used in a paper mill. If the chipper drive is a slip ring induction motor, several advantages arise from using a rheostat in the rotor circuit. This paper will investigate the impact of a rotor circuit rheostat with respect to starting behavior and heavy duty load impulses. Furthermore an alternative chipper drive with a speed controlled squirrel cage induction machine will be presented. Both drives are modeled in Modelica. Simulation results are compared and discussed.

Keywords: Chipper drive; slip ring induction motor; squirrel cage induction machine; speed control; load impulses; simulation model

1 Introduction

Chipper drives are used in paper mills for crushing trunks and making wood chips. The nominal power of a motor used for such applications ranges from several 100 kW up to 2 MW and even more. A chipper drive is usually not operated continuously, because load impulse-arise only if a trunk is shredded. After that, the motor is not loaded until the next trunk is processed. The heavy duty load impulses (double the nominal torque) give rise to large motor currents which cause large voltage drops across the mains impedance. To the regulations of the standards, and the actual configuration and structure of the voltage supply, certain voltage drops (flicker effects) may not be exceeded during impulse load or starting operation. Under some circumstances, the chipper drive even has to start with some remaining parts of a trunk loaded which is a heavy duty condition for the motor.

In the following, two possible chipper drive applications are presented. First, a slip ring motor with rheostat in the rotor circuit and, second, a speed controlled squirrel cage motor is investigated.

1.1 Slip Ring Motor with Additional Resistances

Both, starting the chipper drive and heavy duty operating, cause large currents if no measures are taken. For a motor not being supplied by an inverter, high starting currents arise from the low locked rotor impedance of the induction motor [1]. It is therefore often useful to use a slip ring motor instead of squirrel cage motor. With a slip ring motor an additional rheostat in the rotor circuit can be used to increase the impedance. This gives rise to reduced starting currents and improves the torque speed characteristic with the effect, that reactions of the load impulses on the motor currents and voltage sags are diminished, too.

The significant disadvantages of a slip ring motor with additional resistances in the rotor circuit is the deterioration of efficiency due to additional losses in the external rotor resistances and the high abrasion of the brushes, which gives rise to an increased deposit of brush dust in the motor. This brush dust subsequently increases the risk of isolation breakdown and causes higher costs of maintenance.

1.2 Low Voltage Inverter Supplied Squirrel Cage Motor with Speed Control

An alternative approach which gives rise to reduced starting and load peak currents is a speed controlled inverter drive with squirrel cage motor (Fig. 1).

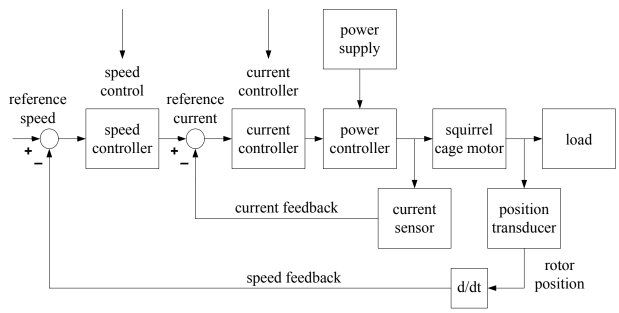

Figure 1: General diagram of a speed controlled drive

The basic topology of a speed controlled drive consists of the electric machine, the power converter, the power supply, cascaded current and speed controller, the mechanical load, the current sensor and the position transducer respectively [2]. The speed controller controls the reference stator current of the machine according to the deviation of the actual speed from the reference speed. The current controller has a build in limitation of the current to avoid overloading the machine. This leads to efficiency savings over a wide operating range and indicates an advantage compared to the realization with a slip ring motor. The higher investment costs due to the additional equipment – the entire speed control implementation with all necessary sensors – are disadvantageous, however.

1.3 Technical Data

Grid	
Frequency	50 Hz
RMS voltage, line-to-line	6000 V
Short-circuit apparent power	50 MVA
Short-circuit power factor	0.05
Transformer's nominal apparent power	1.8 MVA
Transformer's short-circuit p.u. voltage	0.06
Transformer's copper losses	17.5 kW

Table 1: Grid data

Chipper drive with slip ring motor	
Frequency	50 Hz
Number of pole pairs	2
RMS stator voltage, line-to-line	6000 V
RMS stator current	161.1 A
RMS rotor voltage, line-to-line	1500 V
RMS rotor current	595.3 A
Warm stator resistance per phase	129.0E-3 Ω
Stray stator inductance per phase	6.845E-3 H
Main inductance per phase	273.8E-3 H
Stray rotor inductance per phase	0.4631E-3 H
Warm rotor resistance per phase	8.729E-3 Ω
Motor rated power	1.5 MW
Motor rated rpm	1490.8 min^{-1}
Motor inertia	120 $\text{kg} \cdot \text{m}^2$
Load inertia	20000 $\text{kg} \cdot \text{m}^2$
Gear unit	1500:300 min^{-1}

Table 2: Data of the investigated chipper drive with slip ring motor

Chipper drive with squirrel cage motor	
Frequency	50 Hz
Number of pole pairs	2
RMS stator voltage, line-to-line	690 V
RMS stator current	1404.5 A
Warm stator resistance per phase	1.702E-3 Ω
Stray stator inductance per phase	0.10835E-3 H
Main inductance per phase	4.063E-3 H
Stray rotor inductance per phase	0.10835E-3 H
Warm rotor resistance per phase	1.135E-3 Ω
Motor rated power	1.5 MW
Motor rated rpm	1493.9 min^{-1}
Motor inertia	80 $\text{kg} \cdot \text{m}^2$
Load inertia	20000 $\text{kg} \cdot \text{m}^2$
Gear unit	1500:300 min^{-1}

Table 3: Data of the investigated chipper drive with low voltage inverter supplied squirrel cage motor

2 Simulation Models

For performing the Modelica simulations [3] the simulation tool Dymola is used. The behavior of the chipper drive – except for the inverter and control – can be modeled using the comprehensive *Modelica Standard Library* (MSL).

The free MSL provides a collection of standard components and component interfaces for many engineering domains. In the current version of the MSL all components for modeling the proposed chipper drive are offered. For the proposed simulation models mainly the *MultiPhase*, the *Machines* (includes, e.g., direct current, asynchronous induction and permanent magnet synchronous induction machines) and the *Rotational* packages of the MSL are used.

Since the drive controllers are not modeled in the MSL, controlled drives cannot be simulated with components of the MSL, only. Based on the *Machines* library [4] the *SmartElectricDrives* (SED) library [5] facilitates simulations of any electric drive application using different control structures and strategies.

The SED library contains models for the components used in a state-of-the-art electric drive. Sources (batteries and a PEM fuel cell), converters (ideal and power balanced), loads, process controllers, sensors, etc. are provided in this library. In the SED library, two classes of drives simulations are provided. The first class models quasi stationary drives, the second class uses the transient models of the MSL. For fast simulations regarding energy consumption or the efficiency of a drive, the models of the *QuasiStationaryDrives* can be used. They have been modeled with the aim to neglect all electrical transients in the machines. Mechanical transients due to the rotor inertia are considered, however. A great benefit of the *QuasyStationaryDrives* is the remarkable shorter simulation time and the reduced number of input parameters due to simpler controller configuration and the neglect of switching effects. For the analysis of current spikes due to converter switching the *TransientDrives* have to be used. By choosing this lower level of abstraction the user pays the price of more computing time due to a high number of switching events caused by the inverter.

Besides all elementary components that give the user the freedom of building up an entire controlled machine, 'ready to use' models of drives are provided. These models can be used to conveniently and quickly arrange simulations [5]. The '*ready to use*' models contain converters, measurement devices and a *field oriented control* (FOC).

2.1 Slip Ring Motor with Additional Resistances

A slip ring motor with an additional rheostat and an external constant resistance in the rotor circuit can be used to increase the impedance (Fig. 2). This gives rise to reduced starting currents and improves the torque speed characteristic (Fig. 3).

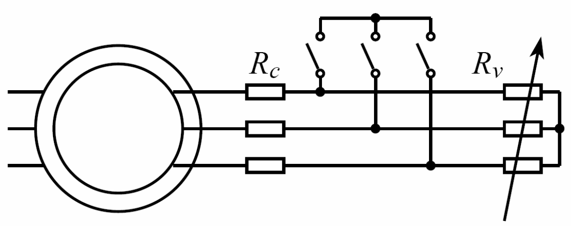

Figure 2: Three phase rheostat of a slip ring induction motor

The total rotor circuit resistance R_r^* consists of the actual rotor (winding) resistance R_r and the external resistance, which in turn consists of the variable resistance of the rheostat R_v and an external constant resistance R_c:

$$R_r^* = R_r + R_v + R_c . \tag{1}$$

During the start-up, the resistance of the rheostat R_v is reduced along a linear ramp. The duration of the ramp has to be chosen according to the actual inertia and starting conditions of the entire chipper drive. After reaching nominal speed, the variable resistance, R_v, is short circuited.

If the motor is not loaded, the resistance R_c does not have a significant influence on the motor current and speed. If the motor is loaded with a constant load torque the stationary speed depends on the actual resistance R_c according to

$$\frac{R_r}{s} = \frac{R_r + R_c}{s_c} , \tag{2}$$

where s denotes the slip for the case without external rotor circuit resistance, and s_c is the slip for the case with the external rotor circuit resistance R_c [6].

The total rotor circuit resistance leads to a scaled torque-slip characteristic. Therefore, load impulses can be covered partially by the stored energy of all rotating masses. The stationary torque speed characteristic of an induction motor is shown in Fig. 3, the stator current versus speed is shown in Fig. 4. For a short circuited slip ring rotor ($R_r^* = R_r$) the torque speed characteristic shows a very low starting torque and a starting current of approximately 5 times the nominal current. For $R_r^* = 21R_r$ the stationary characteristics show a significant improvement. In this case the locked rotor torque is close to the breakdown torque and the locked rotor current is less than 4.5 times the nominal current.

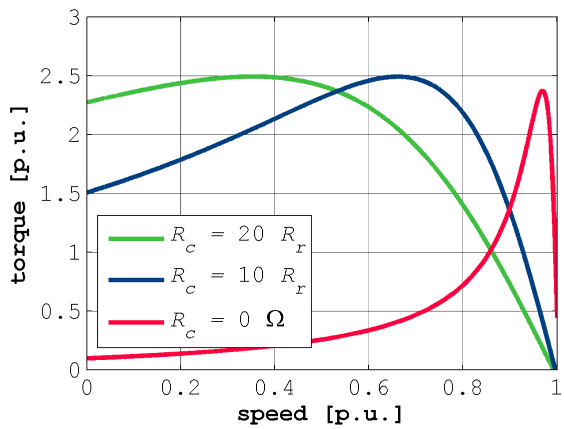

Figure 3: Stationary torque versus speed of a slip ring motor with external rotor resistance

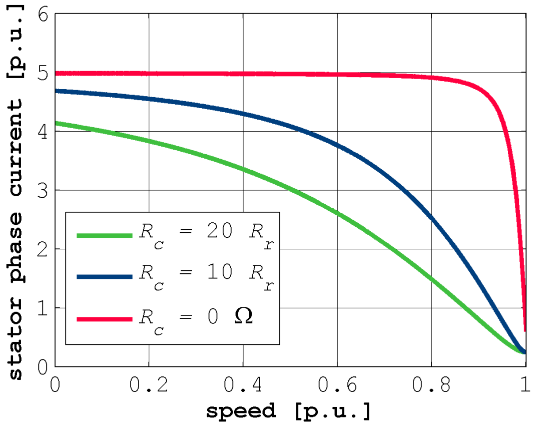

Figure 4: Stationary current versus speed characteristic of a slip ring motor with external rotor resistance

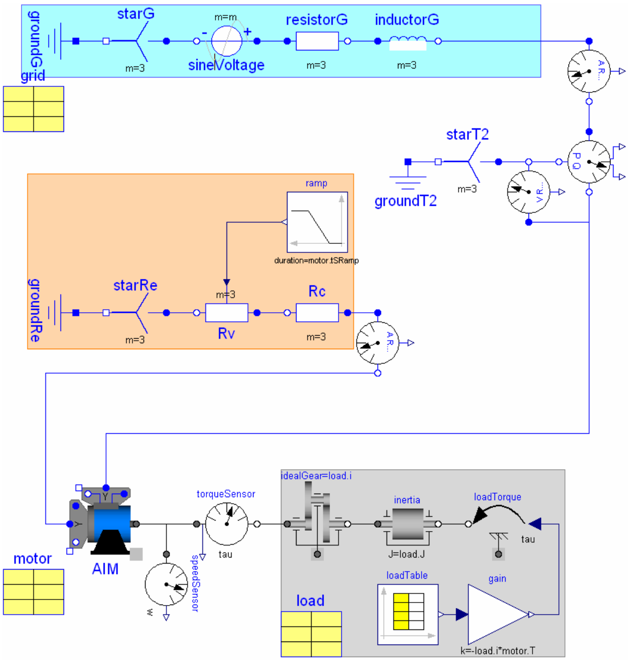

Figure 5: Chipper drive with slip ring motor

Figure 5 depicts the Modelica model of the chipper drive realized with a slip ring motor. The 6 kV / 50 Hz voltage supply is modeled by three sinusoidal supply voltages (`sineVoltage`) which are star (`starG`) connected. The overall mains impedance including all transmission lines and transformers, is modeled by a series connection of a three phase resistor (`resistorG`) and a three phase inductor (`inductorG`). For having the *root mean square* (RMS) values of the voltages and currents in the simulation results available, an RMS voltmeter and amperemeter are connected into the circuit. In addition to these instruments, a power sensor is used to measure the characteristic power terms of the circuit. The stator winding of the slip ring induction motor (`AIM`) is star connected, the stator terminals are connected with the mains impedances, incorporating the instruments for voltage, current and power measurement. The rotor circuit of the slip ring rotor is also star connected. The slip ring terminals are series connected to a constant resistor (`Rc`) and a variable resistor (`Rv`). In the simulation model depicted in Fig. 5 the variable resistor is controlled by a ramp during the start-up of the motor. The signal inputs of the variable resistor, however, can be controlled by any other strategy as well. The mechanical shaft of the induction motor is connected with a torque and speed sensor. The power is transmitted through a gear (`idealGear`) to the load torque (`loadTorque`) model. The signal input of the load torque model is supplied by a time table (`loadTable`) modeling impulse loads.

2.2 Low Voltage Inverter Supplied Squirrel Cage Motor with Speed Control

In Fig. 6 a speed controlled chipper drive with a squirrel cage induction motor is presented. This drive uses components of the SED library. The voltage supply and measurement is the same as in the previous model, except that a transformer is used to provide 690 V to the low voltage drive.

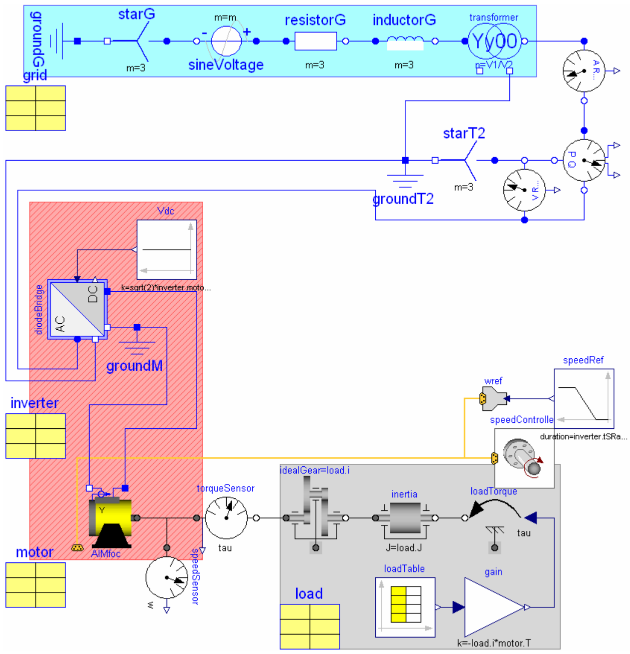

Figure 6: Modelica model of a speed controlled chipper drive with a squirrel cage motor

The transformed supply voltage (`transformer`) is rectified (`diodeBridge`) and provides the intermediate circuit voltage for the inverter. The idealized rectifier does not take into consideration the typical non-sinusoidal waveform of a diode bridge. Therefore the supply current is rather comparable to that of an IGBT rectifier. The squirrel cage induction motor is supplied by a DC/AC-inverter which is implemented in the field oriented controlled *QuasyStationaryDrive* model (`AIMfoc`). The mechanical load model of the slip ring motor and the inverter drive are the same, however.

The components of the cascade control system anticipated in Fig. 1 can be parameterized separately [7]. Starting from the innermost to the outermost closed loop, various parameterization methods can be applied to achieve the desired dynamic behavior [8].

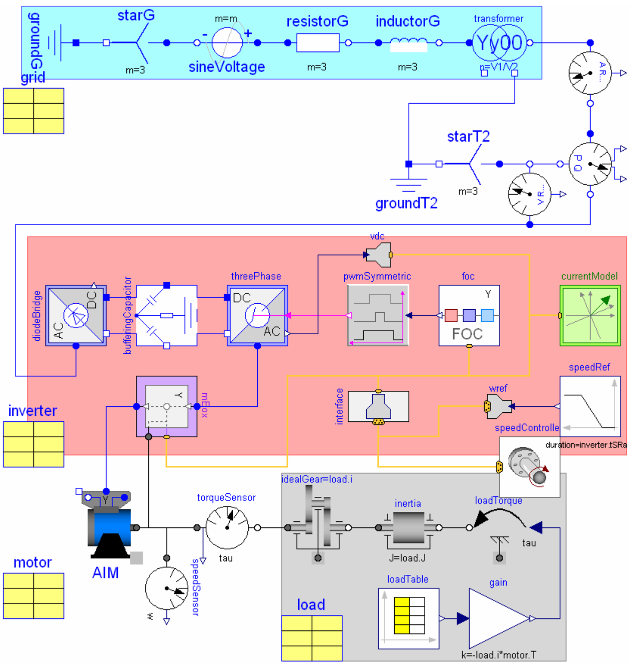

Figure 7: Full transient Modelica model of a speed controlled chipper drive with a squirrel cage motor

In Fig. 7 the full transient Modelica model of a speed controlled chipper drive with a squirrel cage induction motor is presented. This drive uses components of the SED library, again. The voltage supply and measurement is the same as in the quasi stationary model, but using an ideal switching diode rectifier. Additionally, the machine inverter is modeled in detail, not being integrated in the drive model. The detailed model of the ideal switching inverter leads to high number of events during simulation, and gives rise to significantly longer simulation time.

The dominant mechanical time constants are significantly greater than the electrical time constants. Provided that current peaks due to inverter switching may be neglected for this investigation, it is reasonable to use the *QuasiStationaryDrive* model which saves a significant amount of simulation time.

3 Simulation Results

In the presented results each load impulse has the same duration (2 s), equal rise and fall times (0.1 s) and the torque amplitude is twice the nominal torque. The first load impulse starts at $t = 30$ s, the second impulse starts at $t = 40$ s (cp. Fig. 8 and Fig. 12).

3.1 Slip Ring Motor

Simulation results for the chipper drive with slip ring motor are depicted in Fig. 8–11, where $R_c = 0\ \Omega$ and $R_c = 10R_r$ were set consecutively. The duration of the linear ramp for decreasing the variable resistor ($R_{v,max} = 40R_r$) is 10 s. From Fig. 8 and 9 it can be deduced that the torque and current, respectively, get reduced due to the additional resistances in the rotor circuit. The supply current of the slip ring motor drive equals the stator phase current.

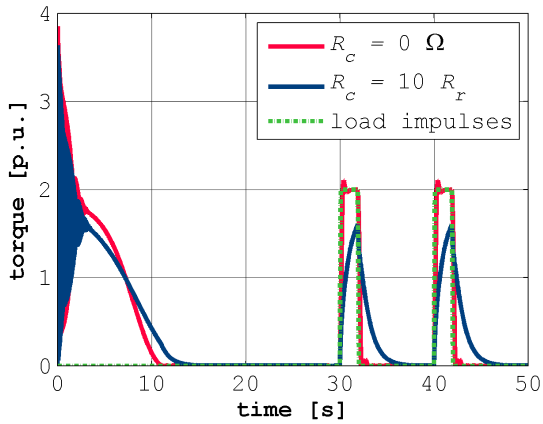

Figure 8: Load response of the slip ring motor ($R_c = 0\ \Omega$ versus $R_c = 10R_r$ and $R_{v,max} = 40R_r$) and wave form of the modeled load impulses

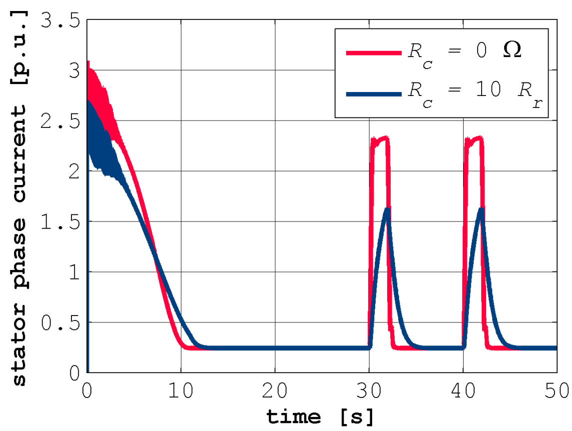

Figure 9: Stator phase current during start-up and during periodic loading of the chipper drive with slip ring motor ($R_c = 0\ \Omega$ versus $R_c = 10R_r$ and $R_{v,max} = 40R_r$)

From Fig. 10 it is evident, that the additional resistance in the rotor circuit decreases the maximum voltage sag at the motor terminals. Figure 11 shows that higher external rotor resistance leads to larger speed drop during the load impulses.

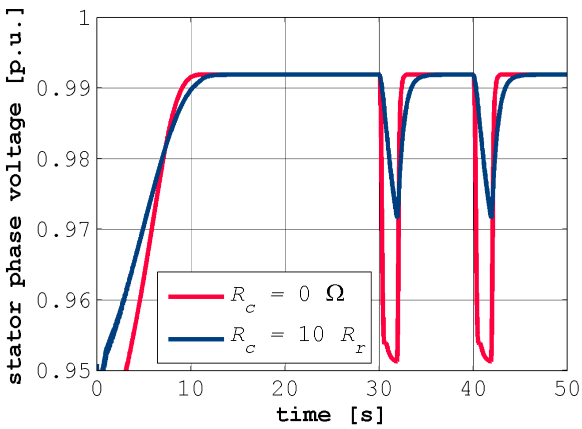

Figure 10: Stator phase voltage during start-up and during periodic loading of the chipper drive with slip ring motor ($R_c = 0\ \Omega$ versus $R_c = 10R_r$ and $R_{v,max} = 40R_r$)

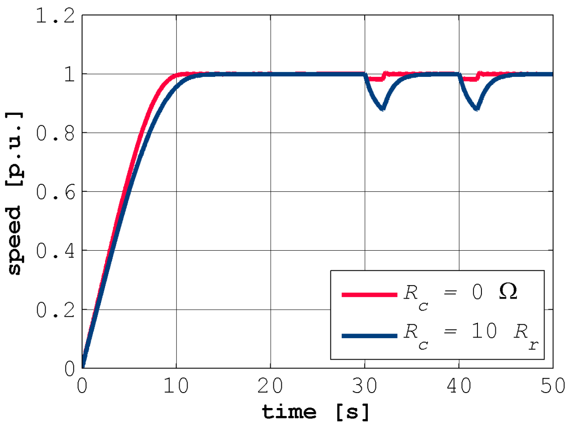

Figure 11: Speed during start-up and during periodic loading of the chipper drive with slip ring motor ($R_c = 0\ \Omega$ versus $R_c = 10R_r$ and $R_{v,max} = 40R_r$)

3.2 Squirrel Cage Motor

Simulation results for the chipper drive with squirrel cage motor are depicted in Fig. 12–15. From Fig. 12 and 13 it can be seen, that the overloading of the machine is limited effectively by the current controller. The diminishing of the supply current peaks shows a significant improvement and the voltage drops are less than 2 % (cp. Fig. 14). Figure 15 illustrates, that the speed drop during the load impulses shows a similar dynamic characteristic as the chipper drive with slip ring motor ($R_c = 10R_r$ and $R_{v,max} = 40R_r$).

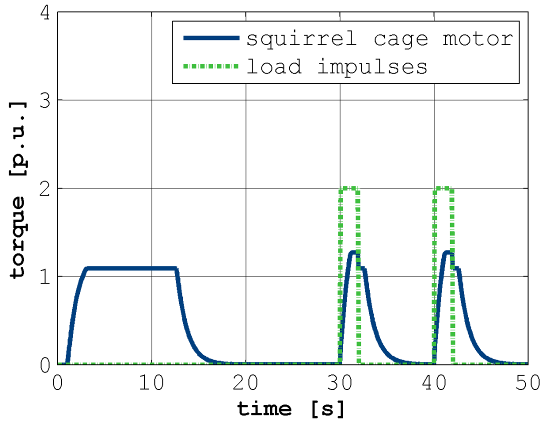

Figure 12: Load response of the speed controlled squirrel cage motor and wave form of the modeled load impulses

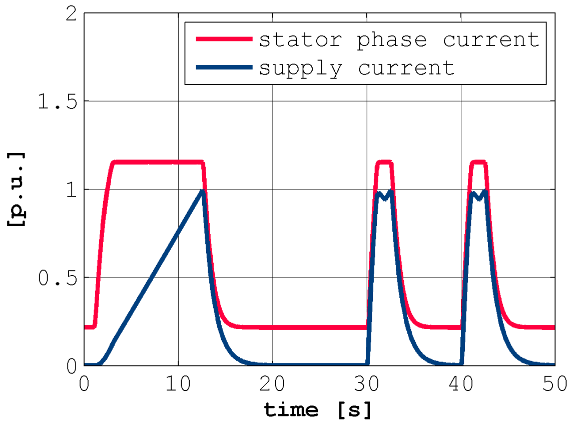

Figure 13: Supply current and stator phase current during start-up and during periodic loading of the chipper drive with speed controlled squirrel cage motor

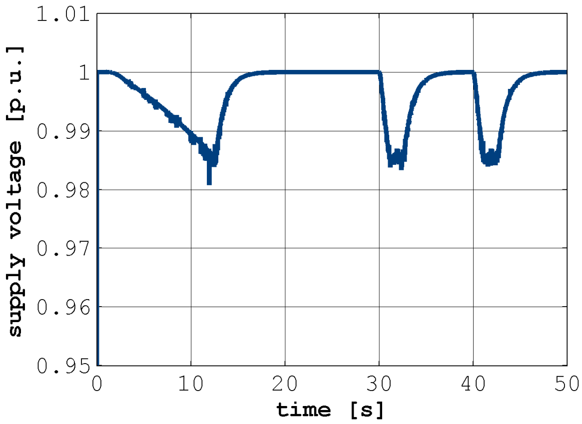

Figure 14: Supply voltage during start-up and during periodic loading of the chipper drive with speed controlled squirrel cage motor

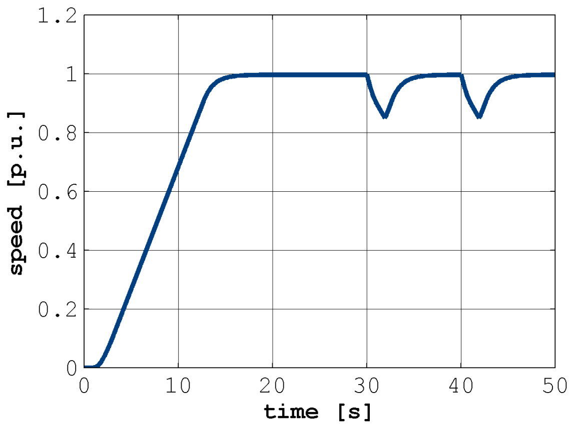

Figure 15: Speed during start-up and during periodic loading of the chipper drive with speed controlled squirrel cage motor

4 Conclusions

In this paper two large chipper drives are modeled in Modelica. The first drive is a slip ring motor with an external resistance in the rotor circuit; the second drive is a speed controlled squirrel cage motor. Both drives lead to a satisfactory reduction of voltage dips and current peaks during the start-up and the pulse load operation.

Using a chipper drive with a slip ring induction motor, the investment costs for the motor are higher than for an induction motor with squirrel cage. In case of the slip ring motor the rather simple additional equipment – the rheostat and its control – leads to low total investment costs.

Disadvantages of the slip ring motor are the deterioration of efficiency due to additional losses in the external rotor circuit and the high abrasion of the brushes, which gives rise to an increased deposit of brush dust in the motor. This brush dust subsequently increases the risk of isolation breakdown and causes higher costs of maintenance.

Contrarily, the inverter drive has lower costs of maintenance but higher investment costs. Although the squirrel cage induction motor is cheaper, more expensive additional equipment is needed: a transformer as well as a frequency inverter and the entire speed control unit with all necessary sensors.

However, the efficiency savings over a wide operating range and the absence of brushes indicates the main advantages compared to the slip ring motor.

References

[1] P. L. Alger, *Induction Machines.* New York: Gordon and Breach Science Verlag, 1970.

[2] S. Nasar and I. Boldea, *Electric Machines; Dynamics and Control.* 2000 Corporate Blvd, USA: CRC Press, 1st ed., 1993

[3] P. Fritzson, *Principles of Object-Oriented Modeling and Simulation with Modelica 2.1.* Piscataway, NJ: IEEE Press, 2004.

[4] C. Kral and A. Haumer, *Modelica Libraries for Dc Machines, Three Phase and Polyphase Machines.* Modelica Conference, 549-558, 2005.

[5] H. Giuliani, C. Kral, J.V. Gragger and F. Pirker, *Modelica Simulation of Electric Drives for Vehicular Applications. The Smart Electric Drives Library.* ASIM, 2005.

[6] R. Fischer, *Elektrische Maschinen.* München: C. Hanser Verlag, 5 ed., 1983.

[7] O. Föllinger, *Regelungstechnik.* Heidelberg: Hüthig Verlag, 8th ed., 1994.

[8] H. Lutz, W. Wendt, *Taschenbuch der Regelungstechnik.* Frankfurt am Main: Wissenschaftlicher Verlag Harri Deutsch, 5th enlarged ed., 2003.